Natural ventilation of a generic cask under a transport hood – CFD and analytical modelling

Daniel Powell, Gavin Davies and Chi-Fung Tso
Arup, London, UK

INTRODUCTION

In comparison with finite element simulation for structural and thermal behaviour, the use of computational fluid dynamics technique (hereafter CFD) to analyse, predict and design air and heat flow in package design is relatively novel.

Arup has been using CFD techniques to investigate fluid and heat flow, and to use it as a tool to design fluid and heat flow across a broad spectrum of industries for over fifteen years. In order demonstrate the power of the technique and its benefits, the airflow and heat flow characteristics around a transport package during transit under a transport hood has been evaluated using the CFD technique. This paper presents the scenario, the model, the analysis technique and the results of this analysis.

Comparison with test results is probably the best way to validate a CFD analysis. In the absence of test results, the analysis was verified by comparison with hand calculation solutions. The scenario as it stands is too complex and hand calculation solution cannot describe the scenario sufficiently. However, hand calculation solutions could be derived for simplified version of the scenario against which CFD analysis of the simplified scenario can be compared. The second half of this paper describes the verification carried out.

DESCRIPTION OF THE SCENARIO

The scenario for the analysis is shown in Figure 1. A loaded spent fuel transport cask is transported under a transport hood.

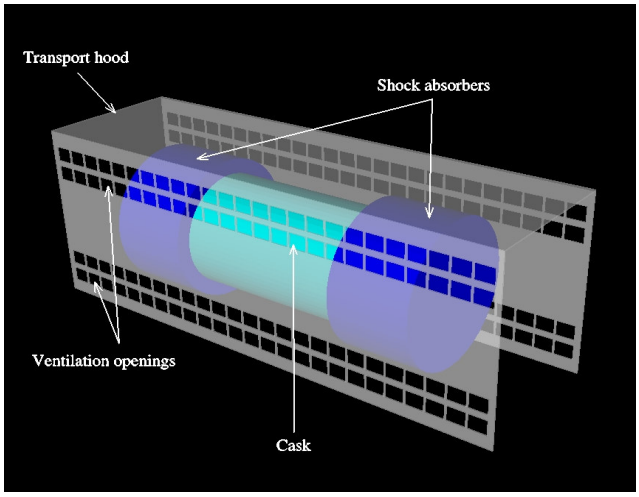

Figure 1: Illustration of the scenario

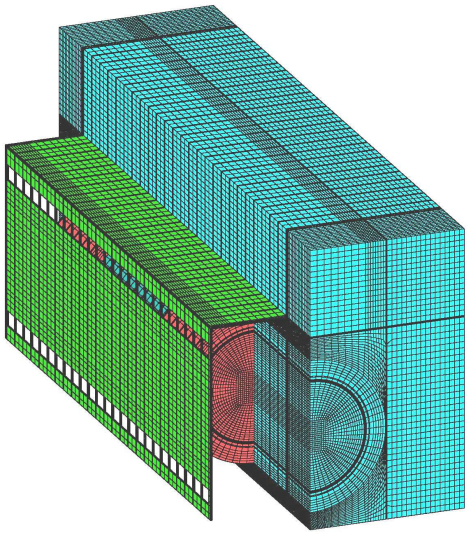

Figure 2: CFD model of the scenario (with part of transport hood and half of the fluid cells blanked from view for clarity)

The cask is cylindrical with an outer diameter of 1.9m. It is fitted with a pair of wood-filled impact limiters, one at each end. Inside the cask is a uniformly distributed heat source with a total power output of 12.6 kW. The total length of the cask assembly is 5.6m.

The transport hood has a collapsible frame structure and is covered with tarpaulin type material. It is 2.5m wide, 8.4m long and 3.1m high. It has open ends and four rows of ventilation openings on each side – two rows near the top and two rows near the base. Each row of vents consists of twenty-five 0.25 x 0.3m openings.

The transport hood is mounted onto the rail wagon, and the cask is secured to the rail wagon by a transport frame. The cask is located centrally in the axial direction and in height under the transport hood. The rail wagon is stationary and there is no wind.

Insolation on the transport hood is taken to be 400 W/m^2 on the top surface and 200 W/m^2 on the vertical surfaces.

METHODOLOGY

The model consisted of the cask, the transport hood and the surrounding exterior environment. It is shown in Figure 2 with part of the mesh cut away to allow the mesh of the transport hood and the cask to be seen. The model consisted of approximately 150,000 solid cells and 600,000 fluid cells.

The cask was given a uniform thermal conductivity of 43 W/mK. Although the steel housing of the shock absorbers would have some effect on the results, for the purposes of this study, they were ignored and the shock absorbers were assumed wooden throughout with a uniform thermal conductivity of 0.15 W/mK.

The hood was given tarpaulin-like material properties, with a uniform thermal conductivity of 0.245W/m. The netting over the ventilation openings was represented as a 78% free area porous opening.

The floor of the vehicle was modelled as an adiabatic surface. The transport frame was ignored – a simplification that is sufficient for the purpose of this analysis.

The external air and ground temperature was assumed to be 311K (38C). All surfaces were assumed to be grey body with an emissivity of 0.93.

A two-equation K-ε model with wall functions was used to model turbulence with the default constants [1]. While it has some limitations, it is currently considered the industry standard.

The model was run initially as a steady state calculation and later changed to a transient calculation. This is often the most efficient way of obtaining a converged solution for problems which exhibit small oscillations about a mean flow and temperature condition. The CFD results presented in this paper are for “snapshots” in time and are representative of the mean flows plus small perturbations. Second order differencing schemes were used for all analyses.

The CFD code StarCD v3.2 [1] was used for the analyses. It is a general purpose Finite Volume Navier-Stokes code widely used in the aerospace, automotive, turbo-machinery, power generation, and building industries.

RESULTS

The airflow has the characteristics of “displacement” ventilation [2] - air entered the hood mainly at low level through the open ends, heated by the heat source within the hood and left mainly through the upper two rows of openings closest to the heat source. The predicted ventilation airflow rates are presented in Table 1, where positive values indicate net flow out of the hood, and negative values indicate net flow into the hood.

	Net Flow rate (kg/s)
High openings – total	+6.0
Low openings – total	+2.0
End openings - total	-8.0

Table 1 – Predicted ventilation rates

Temperature distribution is shown in Figure 3 at four cross-sections along the cask.

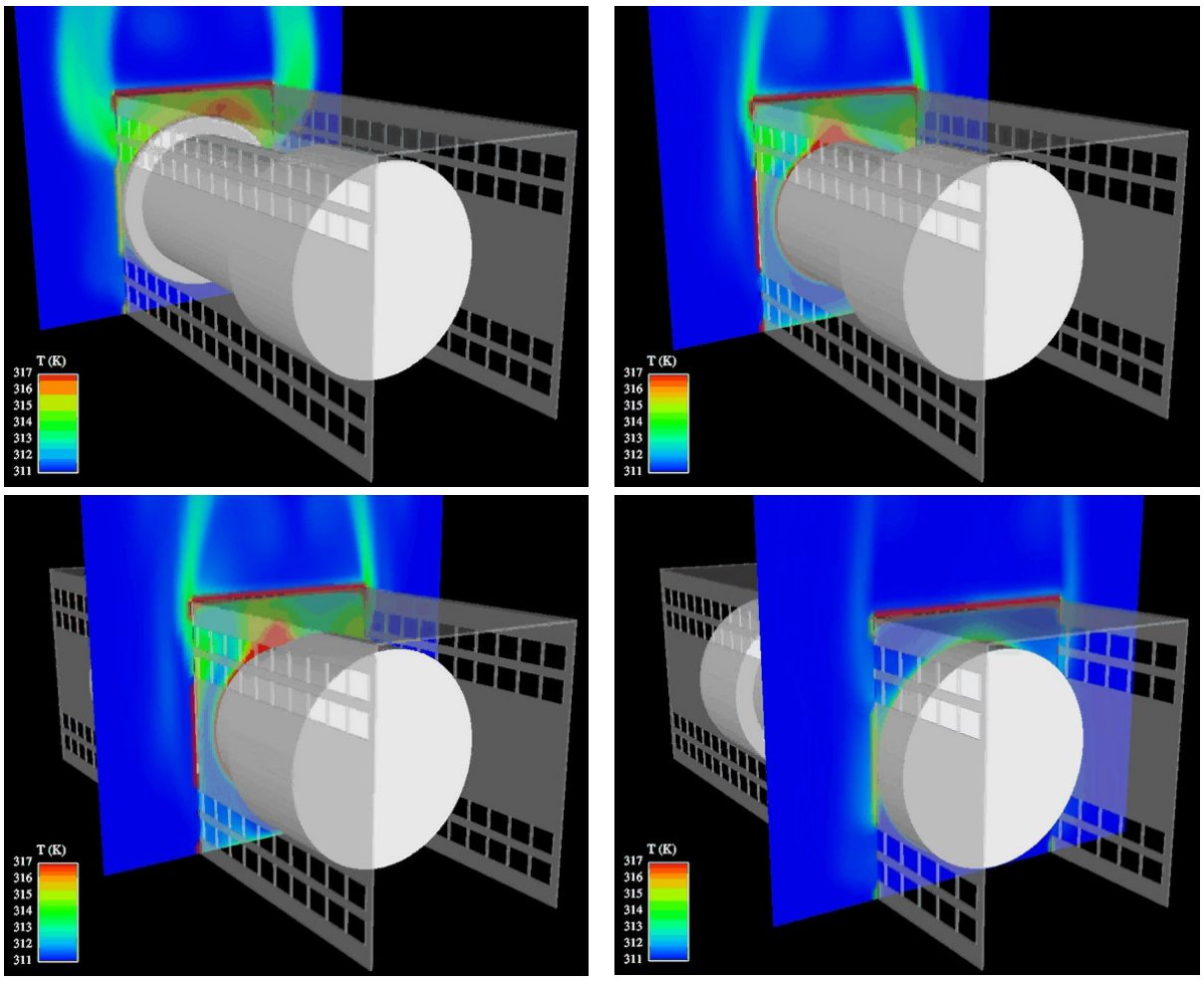

Figure 3: Temperatures distribution at four cross-sections along the package

The highest temperatures around the cask were found above the top of the body due to the stratification produced by the buoyancy driven flow within the hood. The region between the end of the transport hood and the shock absorbers was predicted to be the coolest as this area was well ventilated and has less heat input than the region between the shock absorbers. The analysis predicted a temperature of up to 325K (52℃) occurring close to the top of the cask, and the temperatures within the hood were more typically 313-315K (40 – 42℃). The asymmetry of temperature distribution seen in Figure 3 at the cut-section at mid-length of the cask illustrates the time-dependent instability nature of the flow.

Above the cask, airflow was relatively small and there was some evidence of “short circuiting” with relatively poor ventilation efficiency above the cask.

Surface temperatures of the cask and shock absorbers are shown in Figure 4. The insulating nature of the shock absorbers led to the significantly lower temperatures on their surfaces than on the cask.

Surface temperatures on the outside of the transport hood are shown in Figure 5. The combination of radiant and convective heating from the cask caused the highest temperatures directly above the cask. The effect of radiant heating from the cask to the sidewalls of the hood can also be observed.

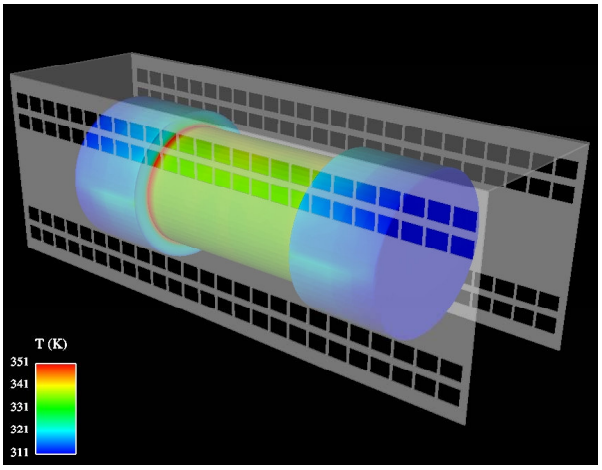

Figure 4: Surface temperatures of the cask and the shock absorbers

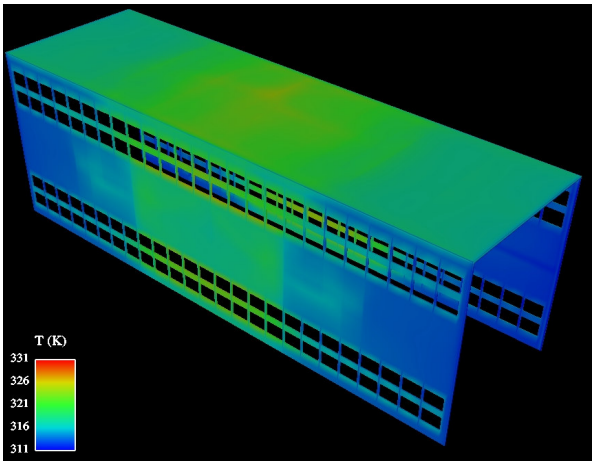

Figure 5: Temperature distribution on the external surfaces of the hood

VERIFICATION OF THE ANALYSIS

The analysis was verified against hand calculation solutions. The scenario as it stands is too complex and hand calculation solution cannot describe the scenario sufficiently. However, if the scenario is simplified, hand calculations solutions could be derived against which CFD analyses of the simplified scenarios can be compared.

Two simplified scenarios were developed from the original scenario and were analysed with the CFD model described above with small modifications to take into account the simplifications. Hand calculation solution for these two simplified scenarios were developed. Results from the CFD analyses and the hand calculation solutions were compared.

SIMPLIFIED CASE 1

Description of the simplified scenario

The ends of the transport hood were blocked off and on each side, one row of ventilation opening at the high level and one row at the low level were blocked. Radiant heat exchange was not considered.

These changes to the scenario allowed the ventilation rate and temperatures to be approximated using a hand calculation approach.

Derivation of the hand calculation solution

The idealised layout of the simplified scenario for deriving the hand calculation solution is shown in Figure 6.

The variables used in the derivation are as follows:

m	mass flow rate of ventilating air /kg/s
Q	heat source from cask /W
H	difference in height between ventilation openings /m
V_1	air velocity in through low level opening /m/s
V_2	air velocity out through high level opening /m/s
dP_1	driving pressure across high level opening /Pa
dP_2	driving pressure across low level opening /Pa
A_0	cross-sectional area of each ventilation opening /m²
K_L	pressure loss coefficient of ventilation openings /dimensionless
T_{INT}	mean internal air temperature /°C
T_{EXT}	external air temperature /°C

ρ_{INT} mean internal air density /kg/m^3
ρ_{EXT} external air density /kg/m^3

dT $T_{INT} - T_{EXT}$
T_c mean temperature of hood /°C
U_c overall heat transfer coefficient for hood /W/m².K
A_c surface area of hood /m²
P_0 ambient air pressure /Pa
R gas constant for air /J/kg.K
C_p specific heat capacity at constant pressure for air /J/kg.K
g acceleration due to gravity /m/s²

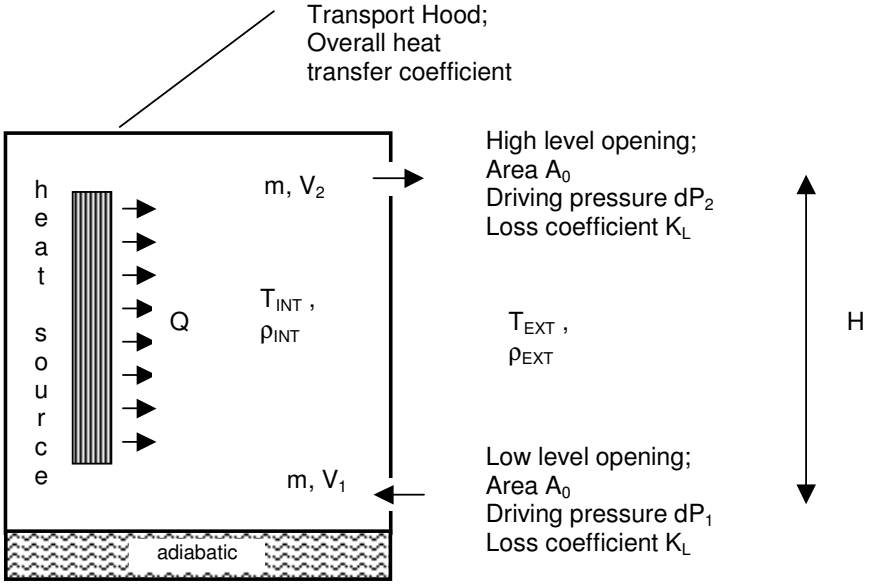

Figure 6: Idealised lay-out of the simplified scenario 1 for derivation of the hand calculation solution

The heat source in the cask is distributed approximately symmetrically about the mid-height of the hood, whilst conduction losses through the hood are not symmetric about this point, these are relatively small for the geometry and conditions considered here. It is therefore reasonable to equate the energy rise in the air as it reaches the mean internal temperature with half of the net heat gains under the hood: -

$$mC_p.dT = ½(Q - UA_c.dT) \quad (1)$$

The pressures which drive the natural ventilation flow are generated by the difference between the internal and external densities, and thus pressure head, of air i.e.: -

$$dP_1 + dP_2 = (\rho_{EXT} - \rho_{INT})gH \quad (2)$$

The driving pressures can also be related to the pressure losses as air flows through the ventilation openings using Darcy's equation [3]: -

$$dP_1 = ½.\rho_{EXT} V_1^2.K_L \quad (3)$$

The velocity of the air through the ventilation opening can be related to the mass flow rate ($V_1 = m/ A_0.\rho_{EXT}$) resulting in the expression: -

$$dP_1 = ½.(m^2/A_0^2.\rho_{EXT}).K_L \quad (4)$$

Similarly, noting that the mass flow rates are the same for both ventilation openings: -

$$dP_2 = ½.(m^2/A_0^2.\rho_{INT}).K_L \quad (5)$$

If (4) + (5) are equated with (2), an expression is generated which relates the mass flow rate to the air densities: -

$$½.(m²/A_0²).K_L.(1/\rho_{EXT} + 1/\rho_{INT}) = (\rho_{EXT} - \rho_{INT})gH \qquad (6)$$

Using the ideal gas equation $P_0 = \rho RT$ and the approximation, $\rho_{EXT} + \rho_{INT} \approx 2\rho_{INT}$, an expression can be derived which relates the mass flow rate to the difference between the internal and external temperature: -

$$m = \rho_{EXT} A_0.[gH.dT./(T_{EXT} K_L)]^{1/2} \qquad (7)$$

Substituting (7) in to (1) yields an expression relating the internal air temperature (i.e. $dT + T_{EXT}$) to the power of the heat source: -

$$2\rho_{EXT} A_0 C_p.[gH/(T_{EXT} K_L)]^{1/2}.dT^{3/2} + UA_c.dT = Q \qquad (8)$$

Assuming the internal and external convective heat transfers are similar, the mean temperature of the hood is given by: -

$$T_c = T_{EXT} + ½.dT \qquad (9)$$

Equations (7), (8) and (9) predict ventilation mass flow rate, internal air temperature and hood temperature respectively.

Comparison of results from CFD analysis and hand calculation solution

dT, m and T_c were calculated using equations [7], [8] and [9] with the following input values: -

Q = 12,600 W; H = 2.35 m; A_0 = 3.75 m²; K_L = 1.5 (see Note 1); T_{EXT} = 38°C; U_c = 2.0 W/m².K; (see Note 2) ; A_c = 88.6 m²; P_0 = 100000 Pa; R= 287 J/kg.K; C_p = 1006 J/kg.K; g = 9.8 m/s²

Notes

1. A loss coefficient of 1.5 is the sum of typical published values for the constituent parts of the vents, a sharp-edged inlet (~0.5) and a sharp edged outlet (~1.0).
2. U value of 2.0 W/m².K is consistent with convective heat transfer coefficients of 5 W/m².K on each side of the hood, this value is an educated estimate consistent with low wind speeds outside the hood however, the results are very insensitive to this quantity so it is of low significance.

CFD analysis of the simplified scenario was carried out using the CFD model of the original scenario but with the ends of the transport hood blocked off, one row of ventilation opening at the high level and one row at the low level on each side of the transport hood blocked, and radiant heat exchange ignored.

Results from the hand calculation solution and the CFD analysis are shown in Table 2. Agreement between the two is good.

Parameter	CFD result	Hand calculation solution result
dT /°C	3.7	3.4
m /kg/s	1.53	1.73
T_c /°C	39.7	39.7

Table 2: Comparison of salient CFD and analytical model results for simplified scenario 1

SIMPLIFIED CASE 2

Description of the simplified scenario

The transport hood was completely removed and radiant heat exchange was ignored. These changes to the scenario allow the application of an empirical expression for natural convection around cylinders.

Derivation of the hand calculation solution

The idealised layout of the simplified scenario for deriving the hand calculation solution is shown in Figure 7. The solution is based on an empirical expression for the heat transfer coefficient of a horizontal cylinder convecting

naturally to an ambient temperature. It assumes that the heat transfer is two-dimensional i.e. 'end effects' are insignificant, and the specific heat capacity, viscosity and conductivity remain constant with varying temperature.

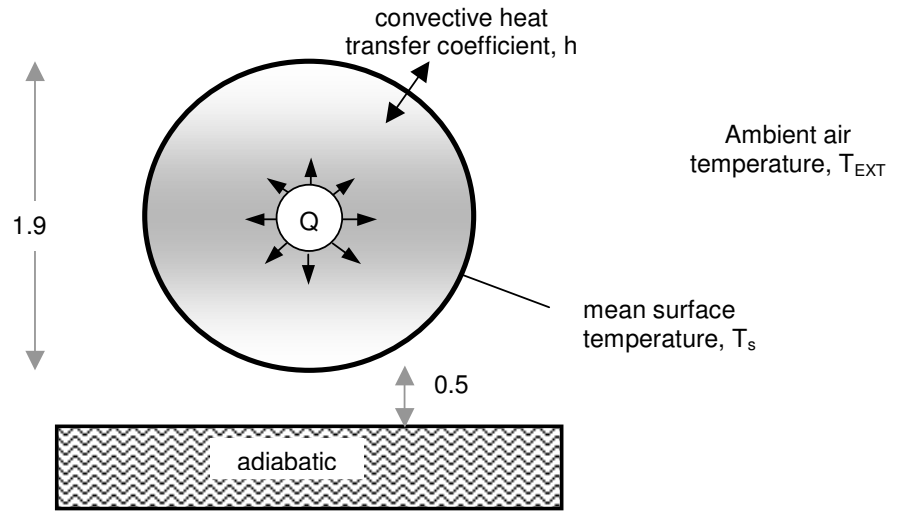

Figure 7: Idealised lay-out of the simplified scenario 2 for derivation of the hand calculation solution

The quantities and variables used in the derivation of the hand calculation solution are as follows:

Q	heat source from cask /W
h	convective heat transfer coefficient at surface of flask /W/m².K
T_s	surface temperature of flask /°C
T_{EXT}	ambient air temperature /°C
Nu	Nusselt number /dimensionless
Pr	Prandtl number /dimensionless
Gr	Grashof number /dimensionless
D	diameter of cask /m
L	is the length of the cask (excluding shock absorbers) /m
k	conductivity of air /W/m.K
β	expansion coefficient of air /K^{-1}
μ	dynamic viscosity of air /Pa.s
C_p	specific heat capacity of air at constant pressure /J/kg.K
ρ	density of air /kg/m³
g	acceleration due to gravity /m/s²
T	$T_s - T_{EXT}$ /°C

Convective heat transfer coefficient of a convecting body is governed by Nu, for horizontal cylinders undergoing natural convection [4]: -

$$Nu = 0.13.(Gr.Pr)^{1/3} \quad (10)$$

and $$h = k.Nu/D \quad (11)$$

where: - $$Gr = \beta g \rho^2 D^3 . dT/\mu^2$$

and $$Pr = C_p \mu /k$$

The surface temperature can then be calculated by equating the heat source with the heat transferred from the surface of the cask i.e.: -

$$T_s = Q/(\pi DLh) + T_{EXT} \quad (12)$$

C_p, μ, and k are assumed to be constant hence Pr is also a constant. β and ρ are functions of temperature and are evaluated at the mean of the surface and ambient temperatures. Consequently, h is also a function of temperature and T_s must be calculated through an iterative process. Evaluation of equations (11) and (12) provides predictions of the convective heat transfer coefficient and temperature on the cask surface.

Comparison of results from CFD analysis and hand calculation solution

T_s and h were evaluated using equations (11) and (12) with the following values:

Q = 8,500 W; T_{EXT} = 38°C; D = 1.94 m; L = 2.94 m; K = 0.0264 W/m.K; μ = 1.81 E-5 Pa.s; C_p = 1,006 J/kg.K; g = 9.8 m/s²

CFD analysis of the simplified scenario was carried out using the CFD model of the original scenario but with the model of the transport hood removed and radiant heat exchange ignored.

The results from the hand calculation solution and the CFD analysis are shown in Table 3 below.

Parameter	CFD result	Hand calculation solution result
T_s /°C	102	116
h /W/m².K	6.9	5.8

Table 3: Comparison of salient CFD and analytical model results for simplified scenario 2

Correlation between hand calculation results and CFD analysis results is reasonable. Some discrepancy between the surface temperatures is expected as the heat flux through the shock absorbers was neglected in the hand calculation solution. However, the main reason for the difference in surface temperatures is the variation in the calculated heat transfer coefficient. In this instance, it is important not to assume that the CFD result is the "right answer" on the basis that the calculation procedure is more complex. Indeed, one of the recognised weaknesses of the turbulence model employed in this analysis is that it tends to over-predict surface heat transfer.

CONCLUSIONS

A CFD study of the airflow and heat flow around a transport cask has been presented. In order to verify the analysis, two simplified scenarios have been developed, analysed by CFD analysis and evaluated by hand calculation solutions.

Agreement between the results of the CFD analysis and the hand calculation solution is generally good. Although neither is a water-tight validation of the other as ultimately both methods are simulations, and neither of the correlation between hand calculation and CFD analysis of the simplified scenarios can be water-tight validation of the original scenario, they do nonetheless increase confidence in the results.

CFD is a versatile technique that can be used on a wide range of flow related scenarios. It is a very powerful tool, if used rightly, can be a robust method to visualise and to understand a flow problem, and to aid the design of packages in scenarios in which fluid and heat flow are significant.

REFERENCES

[1] Computational Dynamics, *StarCD v3.2 – Methodology*, 2004

[2] Linden, P.F., Lane-Serff, G.F. and Smeed, D.A. *Emptying filling boxes: The fluid mechanics of natural ventilation*, J. Fluid Mech. **212**, 300-335, 1990

[3] Howatson AM, Lund PG and Todd JD, *Engineering Tables and Data*, Chapman and Hall, 1991.

[4] Holman JP, *Heat Transfer*, Ninth Edition, McGraw Hill, 2002.